The monocyte chemoattractant protein-1/CCR2 loop, inducible by TGF-β, increases podocyte motility and albumin permeability

Eun Young Lee,[1,2] Choon Hee Chung,[1,3] Charbel C. Khoury,[1] Tet Kin Yeo,[1] Petr E. Pyagay,[1] Amy Wang,[1] and Sheldon Chen[1]

[1]*Division of Nephrology/Hypertension, Northwestern University, Chicago, Illinois;* [2]*Department of Internal Medicine, Soon Chun Hyang University, Cheonan; and* [3]*Department of Internal Medicine, Yonsei University Wonju College of Medicine, Wonju, Korea*

Lee EY, Chung CH, Khoury CC, Yeo TK, Pyagay PE, Wang A, Chen S. The monocyte chemoattractant protein-1/CCR2 loop, inducible by TGF-β, increases podocyte motility and albumin permeability. *Am J Physiol Renal Physiol* 297: F85–F94, 2009. First published May 6, 2009; doi:10.1152/ajprenal.90642.2008.—The role of monocyte chemoattractant protein-1 (MCP-1) in diabetic nephropathy is typically viewed through the lens of inflammation, but MCP-1 might exert noninflammatory effects on the kidney cells directly. Glomerular podocytes in culture, verified to express the marker nephrin, were exposed to diabetic mediators such as high glucose or angiotensin II and assayed for MCP-1. Only transforming growth factor-β (TGF-β) significantly increased MCP-1 production, which was prevented by SB431542 and LY294002, indicating that signaling proceeded through the TGF-β type I receptor kinase and the phosphatidylinositol 3-kinase pathway. The TGF-β-induced MCP-1 was found to activate the podocyte's cysteine-cysteine chemokine receptor 2 (CCR2) and, as a result, enhance the cellular motility, cause rearrangement of the actin cytoskeleton, and increase podocyte permeability to albumin in a Transwell assay. The preceding effects of TGF-β were replicated by treatment with recombinant MCP-1 and blocked by a neutralizing anti-MCP-1 antibody or a specific CCR2 inhibitor, RS102895. In conclusion, this is the first description that TGF-β signaling through PI3K induces the podocyte expression of MCP-1 that can then operate via CCR2 to increase cellular migration and alter albumin permeability characteristics. The pleiotropic effects of MCP-1 on the resident kidney cells such as the podocyte may exacerbate the disease process of diabetic albuminuria.

albuminuria; nephropathy; cytoskeleton; diabetes

MONONOCYTE CHEMOATTRACTANT protein-1 (MCP-1), a member of the cysteine-cysteine ligand chemokine family that regulates the recruitment and activation of monocytes and macrophages, is believed to play a major role in many kidney diseases, including diabetic nephropathy. MCP-1 (also known as CCL2) is upregulated in the diabetic kidney and is excreted in increased amounts in the urine of diabetic subjects (20, 26). The elevation in urinary MCP-1 has been correlated with progression and renal outcomes in humans (1). In culture, various kidney cell lines such as renal tubular cells and mesangial cells have been shown to increase their MCP-1 expression in response to diabetic conditions, as mimicked by high ambient glucose or advanced glycation end products (13). When the MCP-1 increase in diabetes is prevented by a genetic knockout, the mouse model displays amelioration of diabetic albuminuria, reduction in renal fibrosis, preservation of kidney clearance function, and decreased accumulation of macrophages (8). The latter finding of macrophage infiltration in the kidney suggests that diabetic nephropathy can be considered, in part, an inflammatory-mediated disease, and certain immunosuppressive therapies have successfully delayed the development of diabetic renal disease (28).

However, the deleterious actions of MCP-1 in the diabetic kidney may accrue beyond its well-characterized ability to attract macrophages and promote inflammation. The secreted MCP-1 could have substantive effects on the resident kidney cells themselves. The podocyte seems an apt choice for further investigation, as MCP-1 gene expression appears to be predominantly localized to podocytes in the glomeruli of diabetic mice (7), and advanced glycation end products (AGE) stimulate MCP-1 mRNA and protein expression in mouse podocytes (12), raising the possibility that MCP-1 might in turn have a pathogenetic effect on the podocytes. Thus far, it has been shown that the binding of MCP-1 to a specific receptor stimulates the podocyte to enhance its migratory capacity, with possible implications for the progression of crescentic glomerulonephritis (5). Given that the podocyte is subjected to the heightened MCP-1 levels of the diabetic state, further investigation is warranted into the noninflammatory mechanisms whereby MCP-1 participates in the pathogenesis of diabetic nephropathy, especially considering that podocytes play a role in the albuminuria of diabetes.

MCP-1 acts on its target cells by binding to the cognate cysteine-cysteine chemokine receptor 2 (CCR2), a member of the seven-transmembrane, G protein-coupled receptor family that is the main signaling partner of MCP-1 (29). CCR2 probably exists in the podocyte, with mRNA expression demonstrated in glomerular podocytes and CCR2 protein observed in cultured mouse and human podocytes (5, 27). The CCR2 receptor can be inhibited by a nonpeptide molecule dubbed RS102895, which belongs to the structural class of spiropiperidine. The RS102895 compound prevents MCP-1 binding by occupying the interhelical bundle region on the extracellular side of the CCR2 receptor; RS102895 does not antagonize other chemokine receptors such as CXCR1, CCR1, or CCR3 (21). Therefore, RS102895 is a useful tool for interrogating the role of MCP-1/CCR2 signaling in various models of disease.

To isolate the contribution of the podocytic MCP-1/CCR2 system, a cultured line of conditionally immortalized mouse podocytes was utilized. In this study, we determine the diabetic metabolic mediators that can induce MCP-1 expression [e.g., transforming growth factor-β (TGF-β)] and the signaling pathways involved, confirm the expression of CCR2 in podocytes, and establish the paradigm of an inducible podocyte MCP-1/

CCR2 loop. The functionality of this loop, demonstrated by the use of a neutralizing anti-MCP-1 antibody and a CCR2 inhibitor, is evidenced in the significant effects on podocyte motility, the actin cytoskeleton, and the permeability to albumin, phenomena that might underlie the pathophysiology of diabetic albuminuria.

MATERIALS AND METHODS

Cell culture and studies. Conditionally immortalized mouse podocytes derived by Dr. Peter Mundel (University of Miami, Miami, FL) were cultured as previously described (6, 15, 18). The cells were allowed to differentiate for 2 wk at 37.5°C without γ-interferon in DMEM containing 5.5 mM glucose. To characterize the cells, an anti-nephrin antibody and a glutathione S-transferase (GST)-tagged nephrin-blocking peptide (gifts of Dr. Lawrence Holzman, University of Michigan, Ann Arbor, MI) were used in the Western blot procedure, as previously described (6). To examine the effects of diabetic mediators on MCP-1 generation, podocytes were treated with high D-glucose (25 mM), angiotensin II (Sigma), mouse VEGF$_{164}$ (R&D Systems, Minneapolis, MN), or TGF-β1 (R&D Systems). To ascertain the pathways involved in TGF-β-induced MCP-1 production, the following specific inhibitors were added concurrently with the TGF-β1 treatment: a TGF-β receptor kinase inhibitor (SB431542; GlaxoSmithKline, King of Prussia, PA), PI3K inhibitor (LY294002; EMD, San Diego, CA), mitogen-activated protein kinase (MAPK)/extracellular signal-regulated kinase (MEK) inhibitor (PD98059; EMD), or p38 MAPK inhibitor (SB203580; EMD). Antibodies against phospho-Akt (Ser473) and total Akt (Cell Signaling Technology, Danvers,

MA) were used in immunoblotting. To examine the role of MCP-1 signaling, a CCR2 receptor blocker (RS102895; Sigma) or a hamster neutralizing anti-MCP-1 antibody (BD Biosciences, Franklin Lakes, NJ) or preimmune Armenian hamster IgG control was added concurrently with recombinant human TGF-β1 or recombinant mouse MCP-1 (R&D Systems).

As a positive control for the expression of CCR2, a mouse monocyte cell line, WEHI-265.1 (ATCC, Manassas, VA), was grown in suspension in DMEM containing 25 mM glucose and 10% FCS and 0.05 mM 2-mercaptoethanol.

Measurement of MCP-1. The MCP-1 concentration in podocyte lysate was measured using a commercial quantitative sandwich ELISA (R&D Systems) that was specific for mouse MCP-1 and sensitive down to 2 pg/ml. The podocytic MCP-1 concentration was normalized to the total protein concentration.

WST-1 assay for cytotoxicity. A WST-1 assay kit (Cayman Chemical, Ann Arbor, MI) is based on the reduction of a tetrazolium WST-1 salt to soluble formazan by electron transport across the plasma membrane of viable cells (3). Differentiated podocytes grown on a type I collagen-coated 96-well plate at a density of 10^4 cells/well were incubated in serum-free DMEM with 10, 50, and 100 ng/ml of MCP-1 for 24 h. The optical density was measured at 450 nm after incubation with reconstituted WST-1.

Cell motility scratch assay. Podocytes were grown on 35-mm tissue culture plates coated with type I collagen (BD), and the cell monolayer was scratched with a sterile 200-μl pipette tip to create a cell-free, denuded area. Afterward, the culture medium was refreshed and either MCP-1 (50 ng/ml) or TGF-β1 (2 ng/ml) was added, with or without neutralizing anti-MCP-1 antibody (30 μg/ml) or its control:

Fig. 1. Podocyte cell line expresses nephrin. *A*: nephrin protein in the podocyte lysate can be detected by Western blotting at the expected 175- to 185-kDa double immunoband. The nephrin band is competitively diminished by the addition of a nephrin-blocking peptide and unaffected by an irrelevant blocking peptide (BSA); 1:50 refers to the ratio of anti-nephrin antibody to blocking peptide (either nephrin-blocking or irrelevant BSA). β-Actin is shown as a loading control. *B*: nephrin gene expression was verified in podocytes by RT-PCR, using primers that span exons 19 and 22. Mouse kidney total RNA was used as a positive control. Sequencing of the entire 372-bp RT-PCR band was found to match perfectly with the published sequence (accession no. NM_019459). *C*: nephrin by immunofluorescence can be seen to localize preferentially at the cell-cell interface between 3 podocytes in culture (*left*). Nuclei are stained by DAPI. In contrast, nephrin shows less tendency to organize at the margins when the podocyte is solitary (*right*). Magnification: ×400.

Nephrin at the confluence of three podocytes

Nephrin in solitary podocyte

irrelevant Armenian hamster IgG (30 μg/ml) or RS102895 (6 μM). Pictures were taken by inverted microscopy at 0, 24, 36, 42, and 48 h after the scratching procedure, and at each time point the number of cells that had migrated into a uniform-sized rectangular field was counted. The width of the baseline "wound" was quite consistent, averaging 1,114 ± 62 (arbitrary units using Image J software, $n = 24$).

RT-PCR. Podocyte or mouse kidney or monocyte RNA (1 μg), treated first with DNase I to clear any contaminating genomic DNA, was reverse-transcribed in a reaction buffer containing 100 U Super-
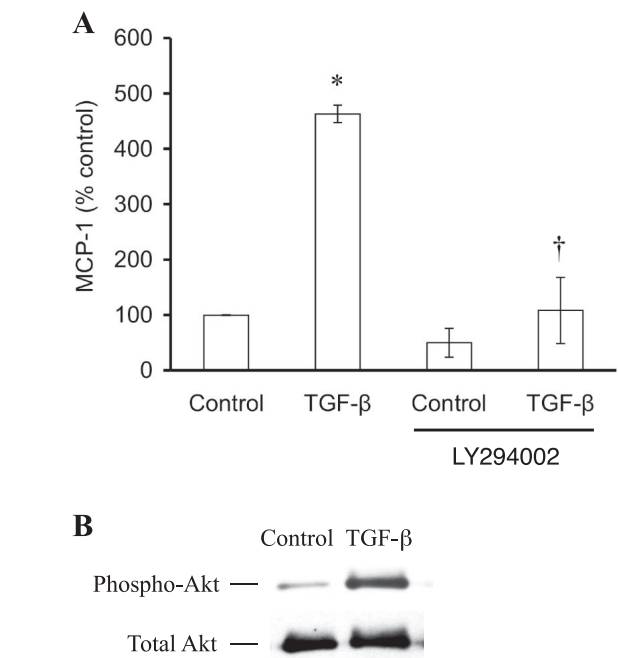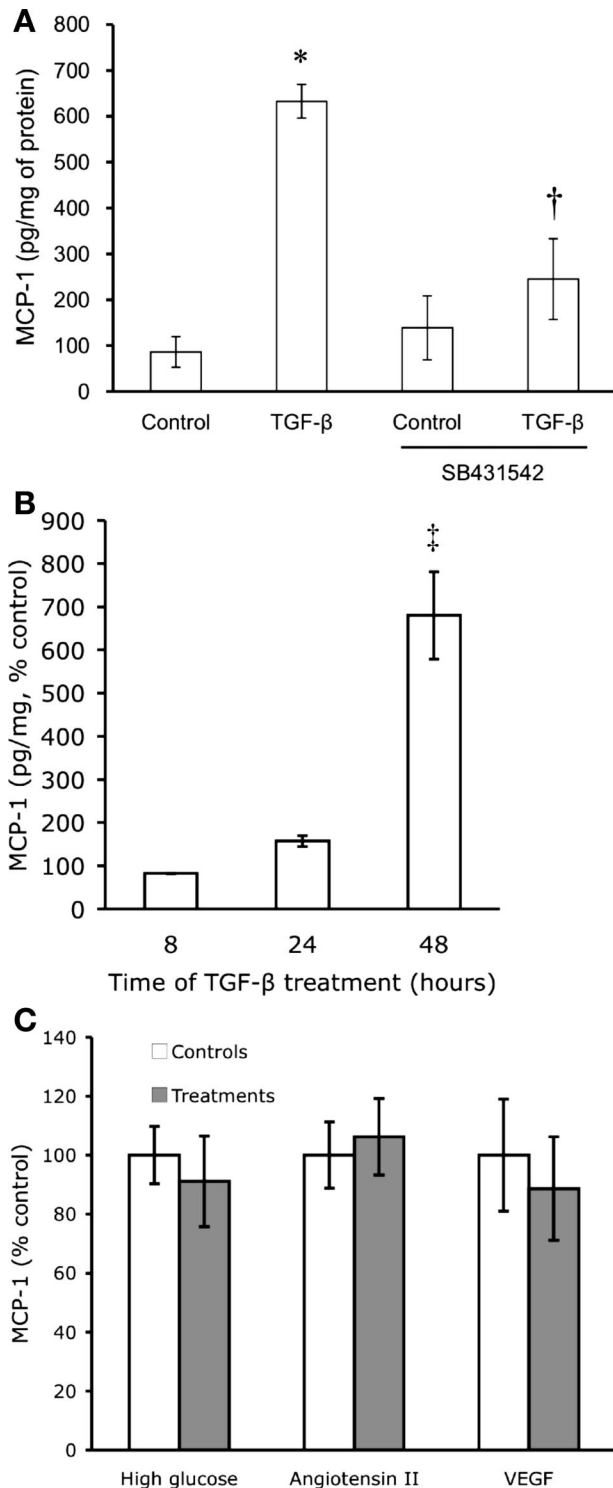
Fig. 3. Phosphatidylinositol 3-kinase (PI3K) mediates TGF-β1-stimulated MCP-1. *A*: a specific inhibitor of PI3K, LY294002 (25 μM), completely inhibited TGF-β-stimulated MCP-1 production by cultured podocytes ($n = 3$). The modest decrease in MCP-1 due to LY294002 alone was not significantly different from control. *$P < 0.05$ vs. control. †$P < 0.05$ vs. TGF-β. *B*: TGF-β1 treatment of podocytes activated the PI3K pathway, evident in the increased amount of phospho-Akt compared with the constant level of total Akt.

script II (Invitrogen, Carlsbad, CA), 0.5 μg gene-specific primer, 20 U RNase inhibitor, and 1 mM dNTPs. The RT reaction was carried out at 42°C for 50 min, followed by inactivation at 70°C for 15 min, after which RNase H was added and the mixture was incubated at 37°C for 30 min. Subsequently, one-fiftieth of the reaction product was added to 20 μl of PCR reaction mix containing 2.5 U *Taq* polymerase (Qiagen, Valencia, CA). As a negative control, distilled/deionized water was used in place of the RNA template. Primers for nephrin RT-PCR were 5'-CCC CAA CAT CGA CTT CAC TT-3' (forward) and 5'-GGC AGG ACA TCC ATG TAG AG-3' (reverse), with a predicted product size of 372 bp using PCR settings as described (31). Primers for CCR2 were 5'-CAC GAA GTA TCC AAG AGC TT-3' (forward) and 5'-CAT GCT CTT CAG CTT TTT AC-3' (reverse) (27), with a predicted product size of 200 bp using PCR settings of initial denaturation at 94°C for 1 min, followed by 30 cycles of denaturation at 94°C for 15 s, annealing at 59°C for 30 s, and extension at 72°C for 30 s, with a final extension at 72°C for 8 min. Aliquots of PCR product were resolved in a 1.5% agarose gel containing ethidium bromide, and photographs under ultraviolet illu-

Fig. 2. TGF-β stimulates monocyte chemoattractant protein-1 (MCP-1) expression. *A*: cultured, differentiated mouse podocytes were treated with 2 ng/ml of recombinant transforming growth factor (TGF)-β1 for 48 h. Compared with control, TGF-β1 markedly increased MCP-1 production as measured by ELISA of cell lysate. The TGF-β-stimulated MCP-1 production was significantly blunted by concurrent treatment with 1 μM SB431542 ($n = 3$). *$P < 0.05$ vs. control. †$P < 0.05$ vs. TGF-β. *B*: TGF-β1 at 2 ng/ml progressively increased podocyte MCP-1 content over time, most evident at 48 h ($n = 5$) when the step-up in MCP-1 production was greatest between TGF-β and vehicle treatment (control for each time point set at 100%). ‡$P < 0.01$ vs. either 8 ($n = 3$) or 24 h ($n = 5$). *C*: high ambient glucose (25 mM) for 2 wk ($n = 4$), angiotensin II (10^{-8} M) for 6 h ($n = 3$), or VEGF (8 ng/ml) for 48 h ($n = 3$) had no significant effects on the production of MCP-1.

mination was captured with a gel documentation system (Fotodyne, Hartland, WI).

Immunofluorescent staining. Podocytes were seeded onto collagen I-coated coverslips and allowed to differentiate for 2 wk at 37.5°C. Coverslips were washed three times in $1\times$ PBS for 5 min apiece. Cells were then fixed in 3.7% formaldehyde for 5 min. Afterward, 0.1% NP-40 in PBS was added for 3 min to permeabilize the cells. Nonspecific binding sites were blocked with 0.1% BSA in PBS for 15 min at 37°C. The coverslips were treated with the following primary antibody solutions at a 1:50 dilution: *1*) anti-CCR2 antibody (Epitomics, Burlingame, CA), *2*) no primary antibody, *3*) anti-CCR2 antibody preadsorbed overnight with 25 times the concentration of CCR2 blocking peptide (Epitomics), *4*) anti-CCR2 antibody preadsorbed overnight with 25 times the concentration of VEGFR-1 (irrelevant) blocking peptide, and *5*) anti-nephrin antibody. After a 1-h incubation at 37°C, the coverslips were washed once in 0.05% Tween 20 in PBS and twice in $1\times$ PBS, and Alexa Fluor 555-conjugated donkey anti-rabbit antibody (Invitrogen) was added at a 1:100 dilution for a 30-min incubation at 37°C in the dark. After one 3-min wash in 0.05% Tween 20 in PBS and two more 3-min washes in PBS, the coverslip was mounted onto a slide in fluorescence mounting medium (Kirkegaard & Perry, Gaithersburg, MD). To visualize filamentous (F)-actin, other podocytes were stained with 2 µM phalloidin-TRITC (Sigma) for 1 h at 37°C. Photomicrographs of randomly chosen sections were taken with a laser-scanning confocal microscope (Zeiss LSM510 META, Göttingen, Germany).

Transwell permeability assay. Podocytes were grown on 3.0-µm-pore Transwell supports (Corning, Lowell, MA) in a 12-well tissue culture plate to form a monolayer, the confluency of which was checked by the measurement of transepithelial resistance (Millicell-ERS by Millipore, Danvers, MA). The experiment was started after the transepithelial resistance had plateaued.

Evans blue-conjugated albumin (EBA; final concentration 0.2 mg/ml) was prepared by diluting a stock solution of 2% Evans blue in a 100-fold excess of 4% bovine serum albumin (25). To measure the permeability of a podocyte monolayer to albumin, EBA was added to the lower chamber of the Transwell and allowed to diffuse into the upper chamber, simulating the movement of albumin from the podocyte's basolateral side to the apical surface. The heights of the media in the upper and lower compartments were kept at the same level, so that bulk flow due to a hydrostatic pressure gradient would not be a factor. During the incubation at 37.5°C, an aliquot of medium from the upper chamber was collected at 24 h, and the EBA was assayed by measuring the absorbance at 620 nm.

Statistical analyses. Data are displayed as means $\pm$ SE for the number of independent experiments indicated in each figure. Student's *t*-test was used to compare two groups. One-way ANOVA followed by multiple comparisons was used to compare multiple groups, such as control and experimental groups, with or without inhibitor (anti-MCP-1 antibody or RS102895). $P < 0.05$ was considered statistically significant.
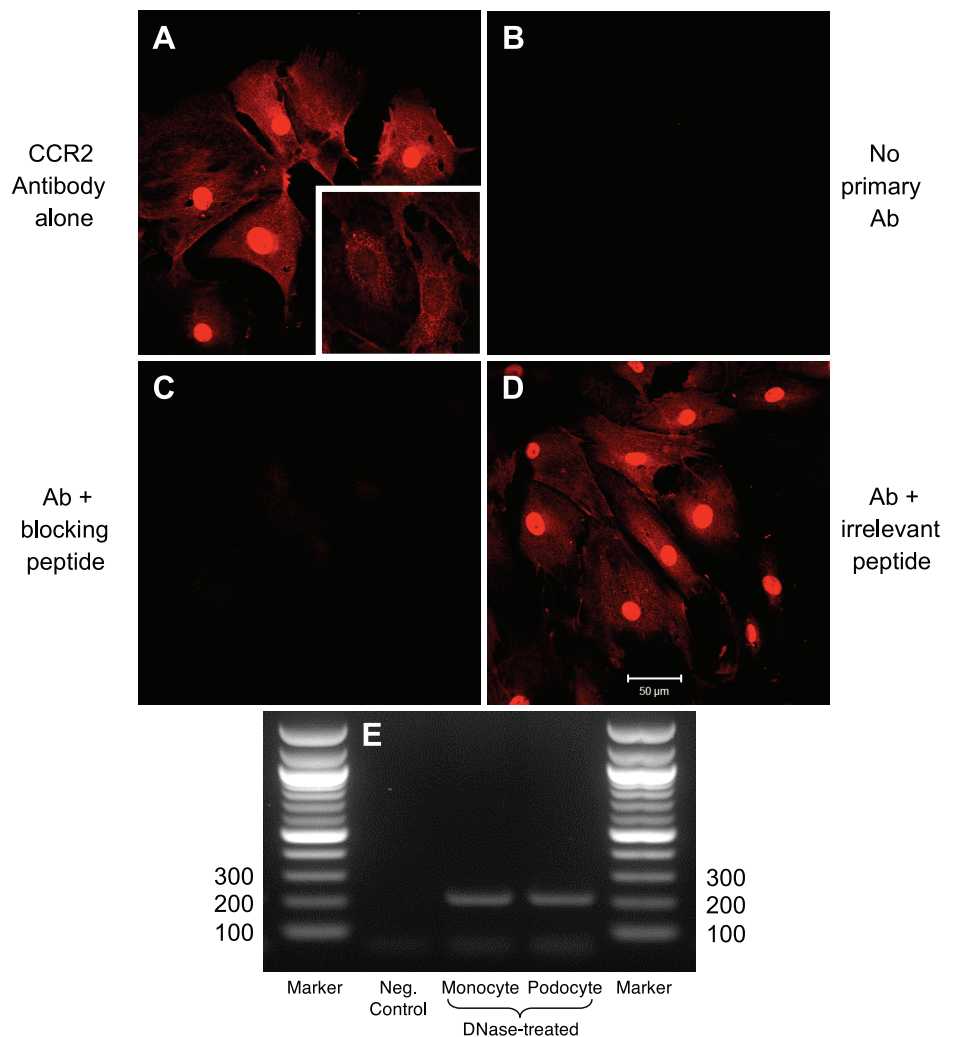
Fig. 4. Cysteine-cysteine chemokine receptor 2 (CCR2) protein and mRNA in podocytes. *A*: CCR2 staining is evident in podocytes as a red signal. The intense nuclear signal abates when the cells are not permeabilized before staining (*inset*). *B*: no fluorescence is detected when the primary antibody is omitted. *C*: staining is competitively obliterated by a blocking peptide, indicating the specificity of the primary antibody for CCR2. *D*: staining is not affected, however, by an irrelevant blocking peptide (in this case, VEGFR-1 antigen). Magnification: $\times 400$. *E*: RT-PCR confirms the expression of CCR2 mRNA in podocytes (200-bp band). RT-PCR performed on monocyte RNA, a positive control, shows a CCR2 band of identical size. The negative control, water, showed no RT-PCR band.

RESULTS

Characterization of podocytes. The conditionally immortalized mouse podocyte cell line (gift of Dr. Peter Mundel) was characterized before experimentation to ensure that we were studying the biology of true podocytes. Our cultured cells expressed synaptopodin, a specific marker of podocyte differentiation (22), but more controversial is whether the cell line expresses nephrin (32). We were able to demonstrate the double immunoband (10) of nephrin at 175–185 kDa on Western blotting, and the specificity of the anti-nephrin antibody (14) was proved by the combination of a blocking peptide that diminished the band's intensity and an irrelevant blocking peptide that left the band unaffected (Fig. 1*A*). No other band on the immunoblot behaved in the same way, and the other nonspecific bands also served as a loading control, along with the β-actin (Fig. 1*A*). To further corroborate the presence of nephrin, its mRNA expression was confirmed in the cell line by RT-PCR that showed a predicted 372-bp band (Fig. 1*B*), which itself was verified by sequencing to match the published cDNA of murine nephrin (accession no. NM_019459, not shown). The water negative control showed no RT-PCR band (not shown). Finally, nephrin protein was visualized by immunocytochemistry at the cell-cell interface between cultured podocytes (Fig. 1*C*, *left*). Solitary podocytes, with no neighbors, did not show a tendency for nephrin to amass at the cell periphery (Fig. 1*C*, *right*).

TGF-β1 stimulates MCP-1 production in cultured podocytes. Cultured podocytes were exposed to exogenous TGF-β1 at 2 ng/ml for 48 h, which significantly stimulated the production of MCP-1 protein as measured by ELISA (7.3-fold higher than control, Fig. 2*A*). The TGF-β1-stimulated MCP-1 production was effectively inhibited by SB431542, an inhibitor of TGF-β signaling (Fig. 2*A*) (17). To characterize the time course of the TGF-β effect, each TGF-β treatment was compared with its respective vehicle control at 8, 24, and 48 h. The effect of TGF-β on podocyte MCP-1 production increased over time and persisted for at least 48 h, a time when the MCP-1 content was noticeably elevated (Fig. 2*B*). Experiments for subsequent figures were thus done at 24 to 48 h.

In addition to TGF-β, other diabetic mediators such as high glucose, angiotensin II, or VEGF were tested for an effect on podocyte MCP-1 production. High glucose (25 mM) for 1 (data not shown) or 2 wk (Fig. 2*C*) did not increase MCP-1 production, and mannitol, an osmotic control for high glucose, also had no effect (data not shown). Similarly, neither angiotensin II (10^{-8} M) nor VEGF (8 ng/ml) significantly affected the production of MCP-1 in cultured podocytes (Fig. 2*C*).

TGF-β1-stimulated MCP-1 is a phosphatidylinositol 3-kinase-dependent pathway. The TGF-β1-induced MCP-1 in podocytes was completely blunted by LY294002 (Fig. 3*A*), implicating phosphatidylinositol 3-kinase (PI3K) as a predominant component of the signaling mechanism. In the absence of TGF-β, LY294002 seemed to depress MCP-1 production, but the difference was not statistically significant. Conversely, TGF-β was able to activate PI3K, seen in the increased phosphorylation of the PI3K substrate, Akt, relative to the total Akt (Fig. 3*B*). In contrast to PI3K, other pathways did not appear to be involved, seen in the lack of effect of PD98059 (inhibitor of extracellular signal-regulated kinase) or SB203580 (inhibitor of p38 mitogen-activated protein kinase) (data not shown).

The CCR2 receptor is present in podocytes. Immunostaining of cultured podocytes was performed and showed a strong fluorescent signal for CCR2 protein (Fig. 4*A*), the negative control of which showed no signal when only the fluorochrome-tagged secondary antibody was used (Fig. 4*B*). Demonstrating the specificity of the primary antibody for CCR2 (Epitomics), an excess of CCR2 blocking peptide was able to competitively abrogate the immunostaining, making the fluorescence virtually undetectable (Fig. 4*C*). The intense homogeneity of the nuclear staining may be artifactual, as much of the signal was attenuated when the podocytes were not permeabilized with NP-40 beforehand (Fig. 4*A*, *inset*). An irrelevant blocking peptide (VEGFR-1 antigen) did not diminish the
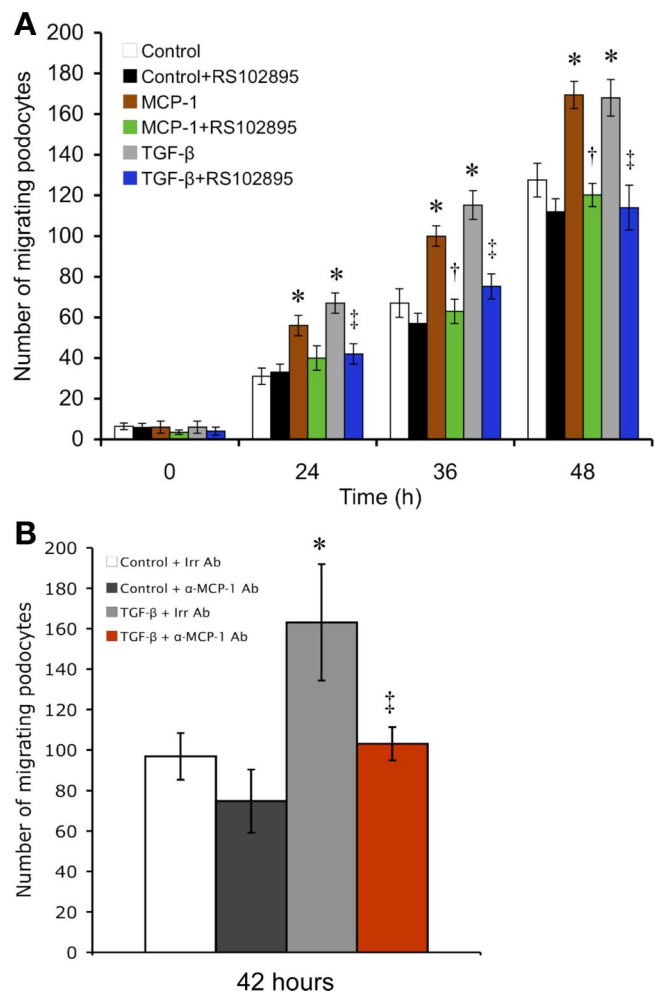
Fig. 5. MCP-1 stimulates podocyte motility as evaluated by a scratch-wound assay. *A*: in the counting of the number of cells that had repopulated a consistently defined area of the scratch, MCP-1 was seen to significantly stimulate podocyte migration at all time points, resulting in quicker wound closure. A similar effect was seen with TGF-β1 treatment. Both MCP-1- and TGF-β1-induced motility increases were prevented by CCR2 inhibition with RS102895 ($n = 4$). *$P < 0.05$ vs. control. †$P < 0.05$ vs. MCP-1. ‡$P < 0.05$ vs. TGF-β. *B*: in a follow-up scratch assay at 42 h, the TGF-β-induced motility gain (gray vs. white bar) was nullified by neutralizing MCP-1 with a specific antibody (α-MCP-1 Ab; red vs. gray bar). A species- and isotype-matched irrelevant antibody (Irr Ab) was used as the control ($n = 3$). *$P < 0.05$ vs. control+Irr Ab. ‡$P < 0.05$ vs. TGF-β+Irr Ab.

immunofluorescence whatsoever (Fig. 4D). Finally, the CCR2 amount by immunostaining did not significantly change with either TGF-β1 or MCP-1 treatment (data not shown).

The gene expression of CCR2 in podocytes was confirmed by RT-PCR. The expected product of 200 bp was seen in podocytes, identical to the band obtained in a monocyte cell line used as a positive control (Fig. 4E). Genomic DNA contamination that might have yielded the same band on the diagnostic gel was ruled out by DNase I treatment before the RT reaction. The water negative control showed no RT-PCR band (Fig. 4E, lane 2).

Exogenous and endogenous MCP-1 increase podocyte motility. Compared with control, MCP-1 treatment caused a podocyte monolayer to fill in a uniform-width scratch wound significantly more quickly at all the time points examined (24, 36, and 48 h, Fig. 5A). TGF-β1 treatment was also able to hasten wound healing (Fig. 5, *A* and *B*). These effects of

TGF-β1 on the podocyte were largely dependent on the MCP-1/CCR2 axis, based on the ability of the anti-MCP-1 antibody (Fig. 5B) or RS102895 (Fig. 5A) to retard cellular migration. However, not all motility is dependent on the MCP-1 system, since treatment to block either MCP-1 or CCR2 still permitted podocyte migration to increase steadily with time (Fig. 5A). There is probably a robust tendency that drives a podocyte monolayer to heal a scratch wound, despite the lack of MCP-1/CCR2 signaling. However, the MCP-1/CCR2 axis is central to the additional motility gains from either MCP-1 or TGF-β stimulation.

MCP-1 causes actin cytoskeleton reorganization. At baseline, untreated podocytes manifested F-actin as cytoplasmic stress fibers, demonstrable by phalloidin-TRITC staining (Fig. 6A). Podocytes treated with MCP-1, however, showed reorganization of the actin filaments from radial stress fibers to peripheral bundles at the cell-cell contacts (Fig. 6B, arrows). A similar
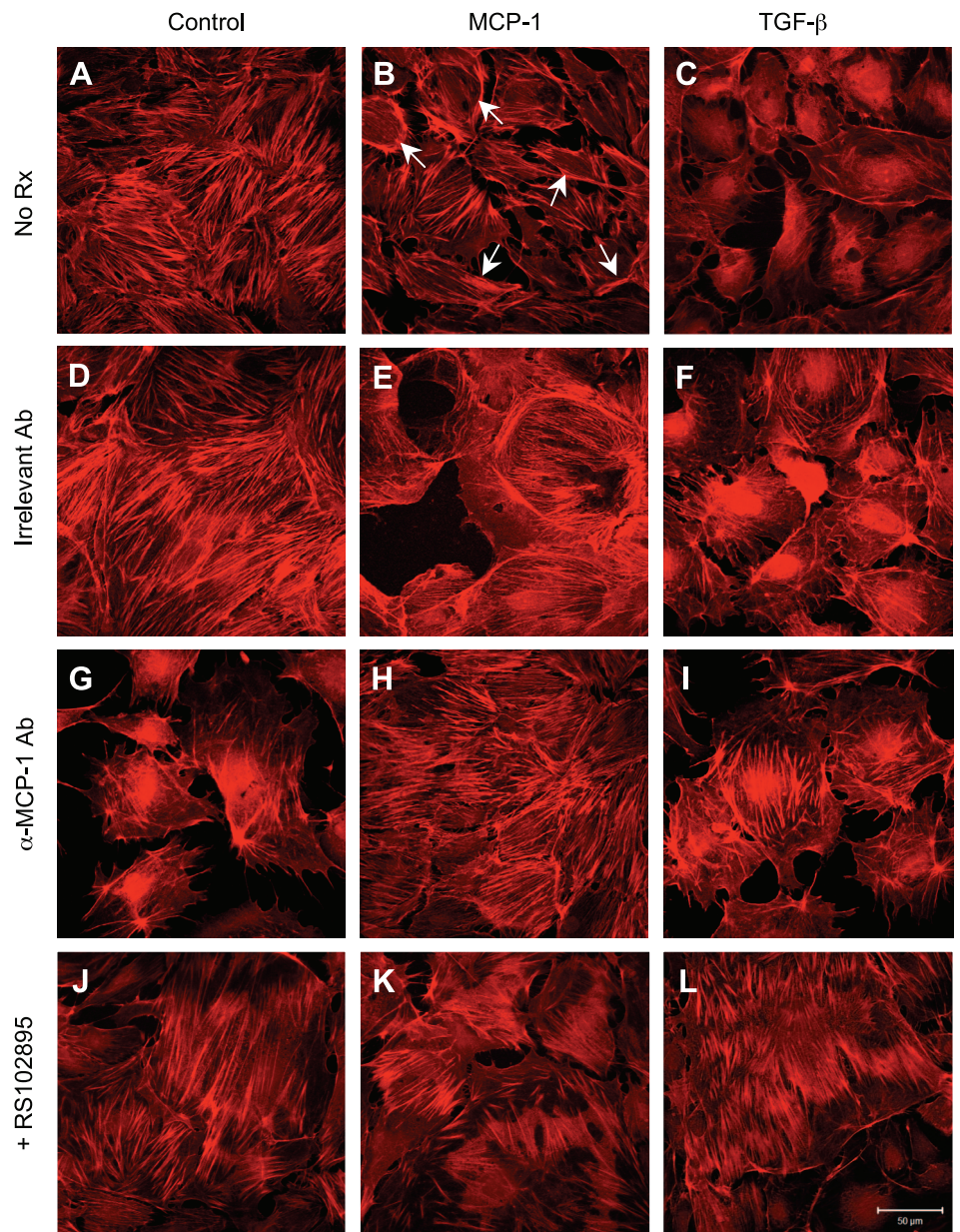
Fig. 6. MCP-1-induced actin cytoskeleton reorganization in podocytes. *A*: filamentous (F)-actin strands were visible as cytoplasmic stress fibers in control cells. *B*: exposure to MCP-1 decreased the density of stress fibers and increased the localization of actin to bundles at the cell periphery (arrows). *C*: TGF-β-treated cells also showed a loss of stress fibers and increased peripheral actin. *D–F*: changes in F-actin appearance described above were not affected by an irrelevant hamster IgG, an isotype control. *G–I*: neutralizing anti-MCP-1 antibody (hamster, 30 μg/ml) greatly reduced the arrangement of F-actin near the cell margins that was secondary to MCP-1 or TGF-β. *J–L*: RS102895 (6 μM), a specific CCR2 inhibitor, also effectively blocked the MCP-1- or TGF-β-induced actin cytoskeletal reorganization. Magnification: ×400.

pattern of F-actin redistribution was recapitulated by TGF-β1 treatment, with slight differences compared with MCP-1 (Fig. 6, *C* vs. *B*). The three F-actin appearances were not altered by an irrelevant hamster IgG, the species- and isotype-matched control for the anti-MCP-1 antibody (Fig. 6, *D–F*). When an antibody was used to neutralize MCP-1, the F-actin staining reverted to a radial pattern in the MCP-1- and TGF-β1-treated podocytes (Fig. 6, *H* and *I*). Similarly, the localization of F-actin near the cell periphery as induced by either MCP-1 or TGF-β1 was prevented by RS102895, a CCR2 receptor inhibitor (Fig. 6, *K* and *L*).

MCP-1 increases podocyte permeability to albumin. Albumin can be tracked in a Transwell apparatus using BSA permanently labeled with Evans blue dye. Since the dye is what is actually assayed, care was taken to remove any free Evans blue not bound to albumin. The spectral absorption profile of Evans blue does not overlap with that of DMEM, the media in which the Transwell experiments were conducted (Fig. 7*A*). The optimal spectrophotometric wavelength for EBA was 620 nm.

To rule out a cytotoxic effect of MCP-1, a cell viability assay using WST-1 reagent (Cayman Chemical) was performed. Podocytes that were treated with 10, 50, or 100 ng/ml of MCP-1 did not demonstrate any cell death at 24 h (data not shown).

Having validated the albumin assay and ruled out cytotoxicity, we measured the albumin permeability of differentiated podocytes using the Transwell setup. After the transepithelial electrical resistance across a podocyte monolayer had plateaued for at least 1 wk (mean: $114.5 \pm 24.6 \ \Omega \cdot cm^2$), treatment with 50 ng/ml MCP-1 for 24 h caused the podocytes to permit increased passage of Evans blue-albumin from the lower to the upper chamber (Fig. 7*B*). Similarly, 2 ng/ml TGF-β1 also increased the permeability to albumin, due to the stimulated MCP-1 release, since blockade of CCR2 signaling by RS102895 could abrogate TGF-β1's effect (Fig. 7*B*). The RS102895 inhibitor also reversed the podocyte's hyperpermeability to albumin due to MCP-1 (Fig. 7*B*). RS102895 appeared to have a greater effect on TGF-β than on MCP-1, but the difference in albumin permeability was not significant between the two or vs. control+RS102895 (Fig. 7*B*).

DISCUSSION

MCP-1 is gaining prominence in the field of diabetic nephropathy and is mainly regarded from the viewpoint of inflammation (36). In general, the action of MCP-1 is to recruit monocytes, T lymphocytes, and basophils to sites of tissue injury and inflammation (29). The kidney in diabetes may be one such locus of inflammation, and both human and animal models of diabetic nephropathy have demonstrated MCP-1 expression in the glomeruli and macrophage accumulation that lead to glomerulosclerosis and progressive renal injury (8, 9). The sources of the renal MCP-1 are diverse and include mesangial cells, tubular epithelial cells, and glomerular epithelial cells, all of which increase their expression of MCP-1 in response to elements of the diabetic milieu (8, 11–13).

Based on the above data, the purpose of renal MCP-1 seems to be to attract inflammatory cells into the kidney parenchyma, but another paradigm that our study suggests is that MCP-1 also possesses noninflammatory effects. In addition to mono-
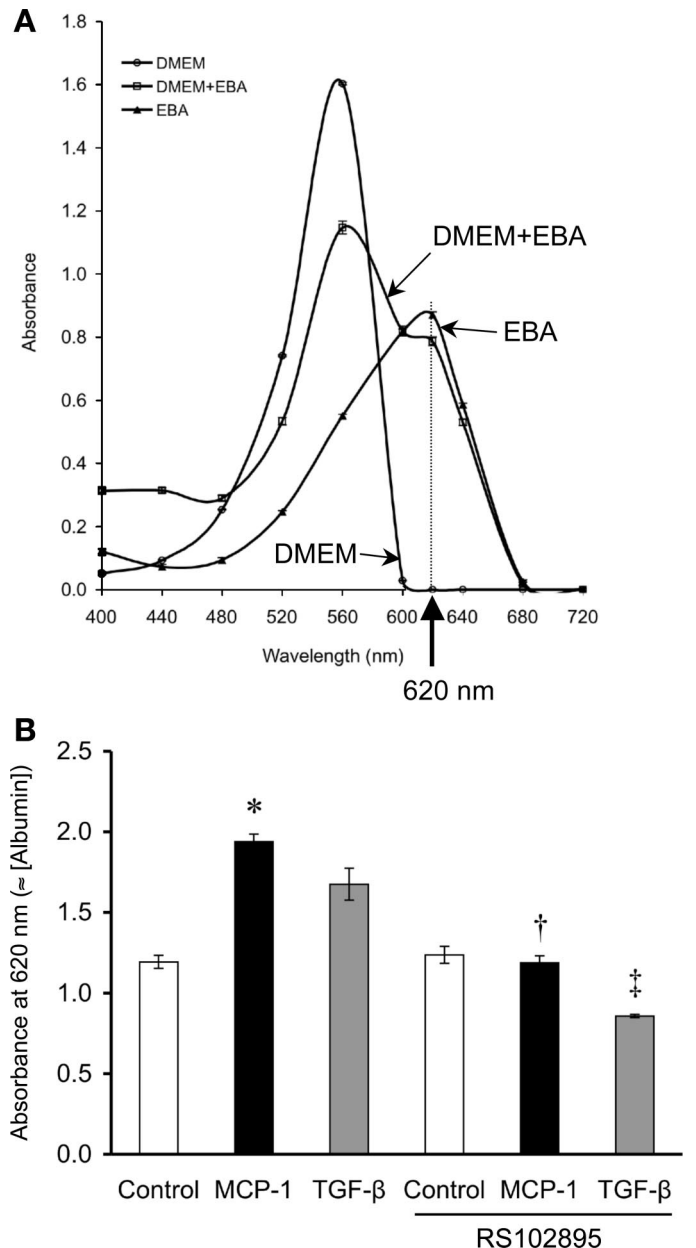

Fig. 7. MCP-1 increases podocyte permeability to albumin. *A*: Evans blue-labeled albumin (EBA) can be quantified by the absorbance characteristics of the Evans blue dye, which absorbs light most strongly at 620 nm. In our tests, the A_{620} measurement is oblivious to DMEM but is quite sensitive to the mixture of DMEM+EBA. *B*: in a Transwell setup to assay the cellular permeability to EBA, performed after the transepithelial electrical resistance had plateaued at $114.5 \pm 24.6 \ \Omega \cdot cm^2$, significantly more EBA had diffused from the lower into the upper chamber across the podocyte monolayer at 24 h as a result of MCP-1 treatment (50 ng/ml) vs. control. TGF-β (2 ng/ml) had a similar effect on EBA transit, although not statistically significant. The permeability to albumin induced by MCP-1 or TGF-β was returned to control levels by concurrent treatment with RS102895 (6 μM), an inhibitor of CCR2 signaling ($n = 4$). $*P < 0.05$ vs. control. $†P < 0.05$ vs. MCP-1. $‡P < 0.05$ vs. TGF-β.

cytes, the targets of the overexpressed MCP-1 in diabetes may be the kidney cells, such as the mesangial cell that responds to MCP-1 via CCR2 by expressing increased amounts of fibronectin and collagen IV (24). Residing in the urinary space, the podocyte certainly has the opportunity to be exposed to

elevated levels of MCP-1, whether they arise from production by the podocytes or other resident glomerular cells. One impact of MCP-1 is to direct the podocytes toward an increased migratory capacity, which was put to good use in the accelerated healing of a scratch wound inflicted on the podocyte monolayer. The power of exogenous MCP-1 to animate podocytes toward efficient wound closure, evident in Fig. 5, was not observed, surprisingly, in a study using human podocytes, even though the cell surfaces adjacent to the wound showed preferential expression of CCR2, suggesting a propensity for the leading edge of the monolayer to migrate into the scratch (5). The podocytes in that study did, however, display chemotaxis/haptotaxis toward an MCP-1 gradient (5). In any case, the MCP-1-induced motility in our study was reflected in the extensive reorganization of the podocyte cytoskeleton, as the actin filaments localized to the leading edges of the cell (Fig. 6).

Could the increased motility represent an adaptive response to the podocytopenia that occurs early on in diabetic nephropathy (34)? Glomerular structure and function would be better served by having the remaining podocytes move to cover up the wound of a basement membrane left bare, mitigating the tendency of the GBM to cohere with Bowman's capsule and contribute to focal glomerulosclerosis (4, 37). Although no in vivo studies have examined whether podocytes actually migrate over the GBM in diabetic nephropathy, the scenario is plausible in that podocytes become more motile in response to osteopontin, and osteopontin expression is highly increased in type 1 diabetes (19). The inevitable morphological changes that accompany increased cell motility might also help explain some of the morphometric observations about the podocyte in diabetes, such as foot process broadening and the decreased slit pore density (23, 35). However, the podocyte migration and altered cytoskeletal dynamics might incur a downside in the form of increased macromolecular permeability of the glomerular filtration barrier, a theory supported by the Transwell data showing that MCP-1 causes increased passage of albumin through a podocyte monolayer (Fig. 7). In vivo, the contribution of MCP-1 to albumin leakage in the kidney has been shown in that albuminuria is significantly ameliorated in the STZ-diabetic mouse by an MCP-1 knockout (8).

One potent stimulus for podocyte MCP-1 expression is TGF-β, a novel finding to the best of our knowledge. The source of TGF-β likely comes from outside the podocyte, as the cell does not produce much TGF-β protein (15), although the podocyte is primed to respond to TGF-β because diabetic mediators upregulate the TGF-β type II receptor that both binds the ligand and initiates the signaling cascade (15, 38). The TGF-β signal that stimulates MCP-1 in the podocyte is dependent on the type I receptor kinase, as demonstrated by the effectiveness of the inhibitor, SB431542. Downstream of the TGF-β type I receptor, the PI3K signaling system (but not ERK or p38) mediates the increase in podocyte MCP-1 production. The PI3K pathway can indeed be activated by the TGF-β receptors (30). Last, the scenario of TGF-β-stimulating MCP-1 production might have in vivo relevance, since renal TGF-β expression is already elevated before the increase in MCP-1 by about a week in the streptozotocin-diabetic mouse model (8, 33).

Once MCP-1 is secreted, it can plausibly diffuse back to the podocyte and act in a loop, by virtue of the CCR2 receptor being present. The existence and operation of such a loop is most convincingly established by the use of an MCP-1/CCR2 antagonist to inhibit the effects of a ligand, TGF-β, that does not even bind to CCR2. It is because TGF-β markedly stimulates the release of endogenous MCP-1 that then binds to and signals through CCR2 that either the anti-MCP-1 antibody or RS102895 compound is effective at inhibiting the increase in cell motility, the concomitant cytoskeletal changes, and the enhanced albumin permeability. That all of these effects can be duplicated by exogenous MCP-1 is further proof that these particular TGF-β-induced behaviors are largely mediated by the podocyte's MCP-1/CCR2 loop. In diabetic mice with nephropathy, CCR2 blockade by a different antagonist, propagermanium, ameliorated mesangial matrix expansion, macrophage infiltration, and overexpression of collagen IV, although the effect on albuminuria was not examined (16). Our discovery of an MCP-1/CCR2 axis in podocytes fits nicely with the recently reported MCP-1/CCR2 system in mesangial cells (24) and with the precedent of a VEGF autocrine loop in podocytes (6), both of which are triggered by TGF-β.

For diabetic podocytopathy, then, the pathogenetic scheme can incorporate a role for the newfound MCP-1/CCR2 loop (Fig. 8). Diabetes provides the high ambient TGF-β in the glomerulus and primes the podocyte to react via upregulation of the TGF-β type II receptor. In a paracrine manner, TGF-β stimulates the podocyte to express MCP-1, via the sequential signaling of the TGF-β type I receptor and PI3K. The released MCP-1 acts back on the podocyte, activating the CCR2 receptor, which initiates profound biological effects. (Of course,

Fig. 8. Proposed TGF-β-induced MCP-1/CCR2 loop in podocytes. *1*: The diabetic milieu stimulates mesangial cells to produce TGF-β. *2*: TGF-β binds to its type II receptor, which is upregulated in the podocytes in diabetes. *3*: Podocytes are stimulated to produce MCP-1 via TGF-β type I receptor signaling and the PI3K pathway. *4*: Via the CCR2 receptor, MCP-1 causes increased podocyte migration, actin cytoskeletal changes, and albumin hyperpermeability.
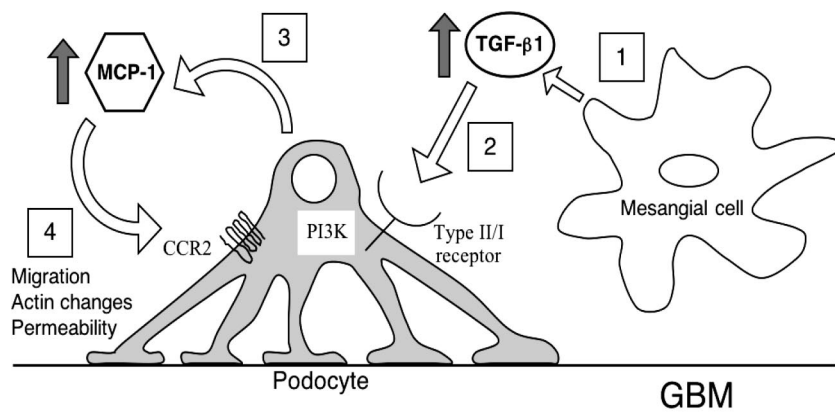
MCP-1 arising from other renal sources could also directly impinge on the podocyte.) Activity of the MCP-1/CCR2 loop causes the podocyte to become more motile, an acquired phenotype reflected in the actin cytoskeletal changes. In the process, the podocyte network becomes more permeable to albumin protein, with potential ramifications for the pathogenesis of diabetic albuminuria. This scenario is supported by the positive correlation between albuminuria and urinary MCP-1 in humans (2). Thus the pleiotropic effects of MCP-1 on noninflammatory cells merit further investigation, and the MCP-1/CCR2 signaling axis might be a potential therapeutic target in diabetic kidney disease (and possibly other renal diseases characterized by an elevated MCP-1 and proteinuria).

REFERENCES

1. **Amann B, Tinzmann R, Angelkort B.** ACE inhibitors improve diabetic nephropathy through suppression of renal MCP-1. *Diabetes Care* 26: 2421–2425, 2003.
2. **Banba N, Nakamura T, Matsumura M, Kuroda H, Hattori Y, Kasai K.** Possible relationship of monocyte chemoattractant protein-1 with diabetic nephropathy. *Kidney Int* 58: 684–690, 2000.
3. **Berridge MV, Herst PM, Tan AS.** Tetrazolium dyes as tools in cell biology: new insights into their cellular reduction. *Biotechnol Annu Rev* 11: 127–152, 2005.
4. **Bondeva T, Ruster C, Franke S, Hammerschmid E, Klagsbrun M, Cohen CD, Wolf G.** Advanced glycation end-products suppress neuropilin-1 expression in podocytes. *Kidney Int* 75: 605–616, 2009.
5. **Burt D, Salvidio G, Tarabra E, Barutta F, Pinach S, Dentelli P, Camussi G, Perin PC, Gruden G.** The monocyte chemoattractant protein-1/cognate CC chemokine receptor 2 system affects cell motility in cultured human podocytes. *Am J Pathol* 171: 1789–1799, 2007.
6. **Chen S, Kasama Y, Lee JS, Jim B, Marin M, Ziyadeh FN.** Podocyte-derived vascular endothelial growth factor mediates the stimulation of alpha3(IV) collagen production by transforming growth factor-beta1 in mouse podocytes. *Diabetes* 53: 2939–2949, 2004.
7. **Chow FY, Nikolic-Paterson DJ, Atkins RC, Tesch GH.** Macrophages in streptozotocin-induced diabetic nephropathy: potential role in renal fibrosis. *Nephrol Dial Transplant* 19: 2987–2996, 2004.
8. **Chow FY, Nikolic-Paterson DJ, Ozols E, Atkins RC, Rollin BJ, Tesch GH.** Monocyte chemoattractant protein-1 promotes the development of diabetic renal injury in streptozotocin-treated mice. *Kidney Int* 69: 73–80, 2006.
9. **Dalla Vestra M, Mussap M, Gallina P, Bruseghin M, Cernigoi AM, Saller A, Plebani M, Fioretto P.** Acute-phase markers of inflammation and glomerular structure in patients with type 2 diabetes. *J Am Soc Nephrol* 16, *Suppl* 1: S78–S82, 2005.
10. **Fujii Y, Khoshnoodi J, Takenaka H, Hosoyamada M, Nakajo A, Bessho F, Kudo A, Takahashi S, Arimura Y, Yamada A, Nagasawa T, Ruotsalainen V, Tryggvason K, Lee AS, Yan K.** The effect of dexamethasone on defective nephrin transport caused by ER stress: a potential mechanism for the therapeutic action of glucocorticoids in the acquired glomerular diseases. *Kidney Int* 69: 1350–1359, 2006.
11. **Gruden G, Setti G, Hayward A, Sugden D, Duggan S, Burt D, Buckingham RE, Gnudi L, Viberti G.** Mechanical stretch induces monocyte chemoattractant activity via an NF-kappaB-dependent monocyte chemoattractant protein-1-mediated pathway in human mesangial cells: inhibition by rosiglitazone. *J Am Soc Nephrol* 16: 688–696, 2005.
12. **Gu L, Hagiwara S, Fan Q, Tanimoto M, Kobata M, Yamashita M, Nishitani T, Gohda T, Ni Z, Qian J, Horikoshi S, Tomino Y.** Role of receptor for advanced glycation end-products and signalling events in advanced glycation end-product-induced monocyte chemoattractant protein-1 expression in differentiated mouse podocytes. *Nephrol Dial Transplant* 21: 299–313, 2006.
13. **Ha H, Yu MR, Choi YJ, Kitamura M, Lee HB.** Role of high glucose-induced nuclear factor-kappaB activation in monocyte chemoattractant protein-1 expression by mesangial cells. *J Am Soc Nephrol* 13: 894–902, 2002.
14. **Holzman LB, St John PL, Kovari IA, Verma R, Holthofer H, Abrahamson DR.** Nephrin localizes to the slit pore of the glomerular epithelial cell. *Kidney Int* 56: 1481–1491, 1999.
15. **Iglesias-de la Cruz MC, Ziyadeh FN, Isono M, Kouahou M, Han DC, Kalluri R, Mundel P, Chen S.** Effects of high glucose and TGF-beta1 on the expression of collagen IV and vascular endothelial growth factor in mouse podocytes. *Kidney Int* 62: 901–913, 2002.
16. **Kanamori H, Matsubara T, Mima A, Sumi E, Nagai K, Takahashi T, Abe H, Iehara N, Fukatsu A, Okamoto H, Kita T, Doi T, Arai H.** Inhibition of MCP-1/CCR2 pathway ameliorates the development of diabetic nephropathy. *Biochem Biophys Res Commun* 360: 772–777, 2007.
17. **Laping NJ, Grygielko E, Mathur A, Butter S, Bomberger J, Tweed C, Martin W, Fornwald J, Lehr R, Harling J, Gaster L, Callahan JF, Olson BA.** Inhibition of transforming growth factor (TGF)-beta1-induced extracellular matrix with a novel inhibitor of the TGF-beta type I receptor kinase activity: SB-431542. *Mol Pharmacol* 62: 58–64, 2002.
18. **Lee EY, Chung CH, Kim JH, Joung HJ, Hong SY.** Antioxidants ameliorate the expression of vascular endothelial growth factor mediated by protein kinase C in diabetic podocytes. *Nephrol Dial Transplant* 21: 1496–1503, 2006.
19. **Lorenzen J, Shah R, Biser A, Staicu SA, Niranjan T, Garcia AM, Gruenwald A, Thomas DB, Shatat IF, Supe K, Woroniecki RP, Susztak K.** The role of osteopontin in the development of albuminuria. *J Am Soc Nephrol* 19: 884–890, 2008.
20. **Mezzano S, Aros C, Droguett A, Burgos ME, Ardiles L, Flores C, Schneider H, Ruiz-Ortega M, Egido J.** NF-kappaB activation and overexpression of regulated genes in human diabetic nephropathy. *Nephrol Dial Transplant* 19: 2505–2512, 2004.
21. **Mirzadegan T, Diehl F, Ebi B, Bhakta S, Polsky I, McCarley D, Mulkins M, Weatherhead GS, Lapierre JM, Dankwardt J, Morgans D Jr, Wilhelm R, Jarnagin K.** Identification of the binding site for a novel class of CCR2b chemokine receptor antagonists: binding to a common chemokine receptor motif within the helical bundle. *J Biol Chem* 275: 25562–25571, 2000.
22. **Mundel P, Reiser J, Zúñiga-Mejía-Borja A, Pavenstädt H, Davidson G, Kriz W, Zeller R.** Rearrangements of the cytoskeleton and cell contacts induce process formation during differentiation of conditionally immortalized mouse podocyte cell lines. *Exp Cell Res* 236: 248–258, 1997.
23. **Pagtalunan ME, Miller PL, Jumping-Eagle S, Nelson RG, Myers BD, Rennke HG, Coplon NS, Sun L, Meyer TW.** Podocyte loss and progressive glomerular injury in type II diabetes. *J Clin Invest* 99: 342–348, 1997.
24. **Park J, Ryu DR, Li JJ, Jung DS, Kwak SJ, Lee SH, Yoo TH, Han SH, Lee JE, Kim DK, Moon SJ, Kim K, Han DS, Kang SW.** MCP-1/CCR2 system is involved in high glucose-induced fibronectin and type IV collagen expression in cultured mesangial cells. *Am J Physiol Renal Physiol* 295: F749–F757, 2008.
25. **Patterson CE, Rhoades RA, Garcia JG.** Evans blue dye as a marker of albumin clearance in cultured endothelial monolayer and isolated lung. *J Appl Physiol* 72: 865–873, 1992.
26. **Qi XM, Wu GZ, Wu YG, Lin H, Shen JJ, Lin SY.** Renoprotective effect of breviscapine through suppression of renal macrophage recruitment in streptozotocin-induced diabetic rats. *Nephron Exp Nephrol* 104: e147–e157, 2006.
27. **Rao VH, Meehan DT, Delimont D, Nakajima M, Wada T, Gratton MA, Cosgrove D.** Role for macrophage metalloelastase in glomerular basement membrane damage associated with Alport syndrome. *Am J Pathol* 169: 32–46, 2006.
28. **Rodriguez-Iturbe B, Quiroz Y, Shahkarami A, Li Z, Vaziri ND.** Mycophenolate mofetil ameliorates nephropathy in the obese Zucker rat. *Kidney Int* 68: 1041–1047, 2005.
29. **Rollins BJ.** Chemokines. *Blood* 90: 909–928, 1997.
30. **Runyan CE, Poncelet AC, Schnaper HW.** TGF-beta receptor-binding proteins: complex interactions. *Cell Signal* 18: 2077–2088, 2006.

31. **Schiwek D, Endlich N, Holzman L, Holthofer H, Kriz W, Endlich K.** Stable expression of nephrin and localization to cell-cell contacts in novel murine podocyte cell lines. *Kidney Int* 66: 91–101, 2004.
32. **Shankland SJ, Pippin JW, Reiser J, Mundel P.** Podocytes in culture: past, present, and future. *Kidney Int* 72: 26–36, 2007.
33. **Sharma K, Jin Y, Guo J, Ziyadeh FN.** Neutralization of TGF-beta by anti-TGF-beta antibody attenuates kidney hypertrophy and the enhanced extracellular matrix gene expression in STZ-induced diabetic mice. *Diabetes* 45: 522–530, 1996.
34. **Steffes MW, Schmidt D, McCrery R, Basgen JM.** Glomerular cell number in normal subjects and in type 1 diabetic patients. *Kidney Int* 59: 2104–2113, 2001.
35. **Sung SH, Ziyadeh FN, Wang A, Pyagay PE, Kanwar YS, Chen S.** Blockade of vascular endothelial growth factor signaling ameliorates diabetic albuminuria in mice. *J Am Soc Nephrol* 17: 3093–3104, 2006.
36. **Tesch GH.** MCP-1/CCL2: a new diagnostic marker and therapeutic target for progressive renal injury in diabetic nephropathy. *Am J Physiol Renal Physiol* 294: F697–F701, 2008.
37. **Toyoda M, Najafian B, Kim Y, Caramori ML, Mauer M.** Podocyte detachment and reduced glomerular capillary endothelial fenestration in human type 1 diabetic nephropathy. *Diabetes* 56: 2155–2160, 2007.
38. **Wolf G, Chen S, Ziyadeh FN.** From the periphery of the glomerular capillary wall toward the center of disease: podocyte injury comes of age in diabetic nephropathy. *Diabetes* 54: 1626–1634, 2005.